# Inhibition of *O*-GlcNAcase by a *gluco*-configured nagstatin and a PUGNAc–imidazole hybrid inhibitor†

**Bhagavathy Shanmugasundaram,[a] Aleksandra W. Debowski,[b] Rebecca J. Dennis,[c] Gideon J. Davies,[c] David J. Vocadlo[b] and Andrea Vasella*[a]**

***Received (in Cambridge, UK) 23rd August 2006, Accepted 11th September 2006***
***First published as an Advance Article on the web 29th September 2006***
**DOI: 10.1039/b612154c**

**Synthesis of a PUGNAc–imidazole hybrid and its characterization as an inhibitor of human *O*-GlcNAcase through enzyme kinetics and X-ray structural analysis.**

The substitution of serine and threonine residues of nucleocytoplasmic proteins with 2-acetamido-2-deoxy-β-D-glucopyranose (*O*-GlcNAc) residues is an essential post-translational modification found within all multicellular eukaryotes.[1–3] Many classes of proteins are modified with *O*-GlcNAc.[2,3] Accordingly, *O*-GlcNAc has been implicated in several disease states such as type II diabetes.[4]

A dynamic balance of cellular *O*-GlcNAc levels is maintained by two carbohydrate processing enzymes. *O*-GlcNAc is removed from modified proteins and returned to their unmodified state by a family‡ 84 glycoside hydrolase known as *O*-GlcNAcase.[5] The structure of a β-*N*-acetylglucosaminidase (*Bt*GH84) from *Bacteroides thetaiotaomicron* has been determined. It reveals an active site in which all but one amino acid residues are conserved compared to the hydrolase domain of human *O*-GlcNAcase.[6] This structural and functional conservation is reflected in the similarity of the inhibition profiles of human *O*-GlcNAcase and *Bt*GH84, making this enzyme a valuable model.[6]

The development of inhibitors of *O*-GlcNAcase as research tools is a topic of interest since the biological roles of *O*-GlcNAc remain ill defined. *O*-(2-acetamido-2-deoxy-D-glucopyranosylidene)amino *N*-phenyl carbamate (PUGNAc, Fig. 1, **1**[7]) is a potent inhibitor ($K_I \approx 50$ nM for human *O*-GlcNAcase[5,8]) that has been used to uncover the function of *O*-GlcNAc at the cellular level.[4] This inhibitor has been proposed on the basis of structural analysis[9] to be a transition state mimic for *O*-GlcNAcase. The *N*-phenyl carbamoyl group of PUGNAc captures significant binding energy since LOGNAc (2-acetamido-2-deoxy-D-glucohydroximo-1,5-lactone, Fig. 1, **2**[7]), an analogue lacking this group, is a considerably weaker inhibitor ($K_I$ = 1.7 μM).[5] Another important structural feature of PUGNAc is the oxime nitrogen that engages in a favourable hydrogen bond with the catalytic acid group.[9] Although PUGNAc is a potent inhibitor, its instability in acidic solutions is a drawback for its use as a research tool.

The natural product nagstatin[11] is a potent inhibitor of β-hexosaminidases and a very stable molecule characterized by the key structural motif of a tetrahydroimidazo[1,2-*a*]pyridine ring system. It is the imidazole moiety and not the carboxymethyl group that is at the origin of the inhibitory potency of the *gluco*-configured analogue of nagstatin (Fig. 1, **3**) toward β-hexosaminidases.[10] Related imidazoles, and similarly stable tetrazoles,[12] are likewise potent inhibitors of a wide range of β-glycosidases.[13,14] Two factors have been advanced to rationalize the potency of these imidazoles. The first is the similarity of the $pK_{(HA)}$ values of the protonated imidazole and of the enzymic general acid catalyst, resulting in a strong hydrogen bond between the imidazole and the catalytic acid,[15] and the second one is the enhanced interaction of the protonated imidazole with the catalytic nucleophile.[16]

In consideration of these features, we engaged in a rational design of stable inhibitors of human *O*-GlcNAcase with increased potency and synthesized the novel PUGNAc–imidazole hybrid inhibitor **4** (Fig. 1). The route we followed (Scheme 1) continued on from an intermediate within a route established for the preparation of substituted tetrahydroimidazopyridines.[17] Condensation of **5** with 2-aminoacetaldehyde dimethylacetal followed by acid catalysed cyclisation in the presence of $H_2O$ afforded cleanly the *gluco*-imidazole **6** (90%). Treatment of **6** with NIS (10 equiv.) in DMF gave the 2,3-diiodoimidazole **7**. Regioselective deiodination at *C*(3) of **7** with EtMgBr (1.0 equiv.) at 0 °C gave the desired 2-iodoimidazole **8**. Addition of PhNCO to the organomagnesium derivative of **8** led to the (phenylcarbamoyl) *gluco*-imidazole **9**, which upon desilylation with $Bu_4NF$ gave the hydroxy-imidazole **10** (58% from **6**).

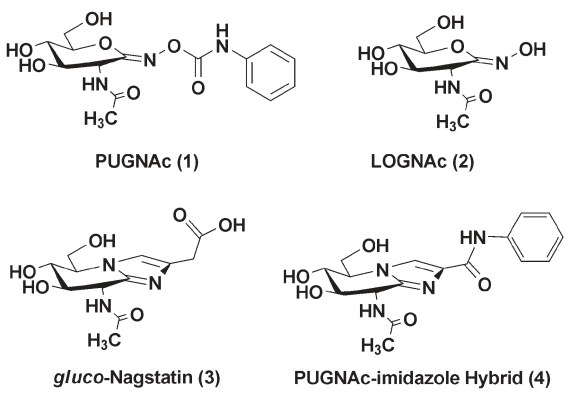


**Fig. 1** Structures of inhibitors discussed.

[a]*Laboratorium für Organische Chemie, HCI H 317, ETH Zürich, CH-8093 Zürich, Switzerland. E-mail: vasella@org.chem.ethz.ch; Fax: +41 1 632 11 36; Tel: +41 1 632 45 16*
[b]*Department of Chemistry, Simon Fraser University, 8888 University Drive, Burnaby, Canada. E-mail: dvocadlo@sfu.ca; Fax: +1 604 291 3765; Tel: +1 604 291 3530*
[c]*Department of Chemistry, The University of York, Heslington, York, UK YO10 5YW. E-mail: davies@ysbl.york.ac.uk; Fax: +44 1904 328266; Tel: +44 1904 328260*

† Electronic supplementary information (ESI) available: Experimental details of the synthesis of **4**, details for the inhibition assays, and X-ray crystallographic studies. See DOI: 10.1039/b612154c

 

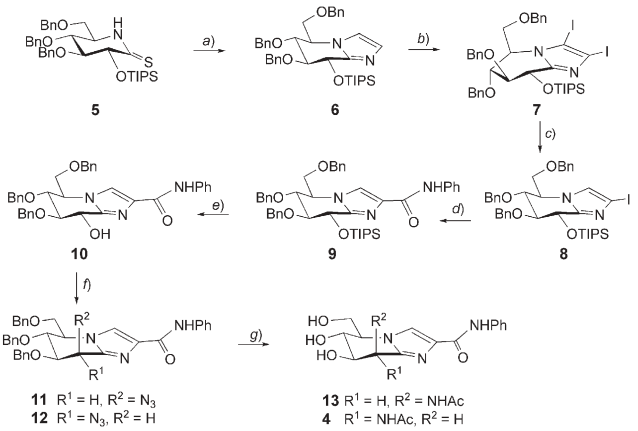

**Scheme 1** *a*) 1. $H_2NCH_2CH(OMe)_2$, $Hg(OAc)_2$, THF; 2. *p*-TsOH·$H_2O$, toluene–$H_2O$; 90%. *b*) *N*-Iodosuccinimide, DMF, 80 °C; 88%. *c*) EtMgBr, THF; 88%. *d*) EtMgBr, then PhNCO, THF; 81%. *e*) 1 M $Bu_4NF$, THF; 93%. *f*) Diphenyl phosphoryl azide (DPPA), DBU, toluene; 85%. *g*) 1. Pd/C, 6 bar of $H_2$, AcOH; 2. $Ac_2O$–pyridine; 3. $NH_3$, MeOH; 23% of **13**; 17% of **4**.

The hydroxy group of **10** was substituted by an azido group using diphenyl phosphorazidate (DPPA) and DBU[10,18] at 55 °C in toluene to yield 85% of an inseparable mixture of the azides **11/12** (2 : 3). Performing the reaction at room temperature afforded the phosphodiester of the alcohol **10**. The presence of an azido group in **11/12** was confirmed by a strong IR band at 2110 $cm^{-1}$. Hydrogenation of the mixture of the azido-imidazoles **11/12** (Pd/C, AcOH) followed by acetylation ($Ac_2O$, Pyr.) and *O*-deacetylation led to a mixture of the epimers **13/4** (≈ 1 : 1) (41%) that were separated by reverse phase HPLC. (See the supporting material).

The *C*(8)–OTIPS diiodo-imidazole **7** probably adopts a conformation in between $^6H_7$ and a sofa conformation similar to the *C*(8)–OBn *gluco* diiodo-imidazole,[17] as evidenced by the vicinal coupling constants *J*(5,6), *J*(5,CH) (1.6, 4.6, respectively). The *C*(8)–OTIPS protected *gluco* configured imidazoles **6** and **8** adopt (in $CDCl_3$) a $^{5,8}B$ conformation with *C*(8)–O in a *pseudo*-axial position, as evidenced by *J*(5,6), *J*(6,7) and *J*(7,8) of ~8.8, ~3.0 and ~3.0, respectively, while **9**, with *J*(6,7), *J*(7,8) (5.0, 5.0), probably adopts a conformation in between boat and $^6H_7$. The *gluco* and *manno* imidazoles **10–13** and **4** adopt a $^6H_7$ conformation. Assignment of the *manno* and *gluco* configuration to **13** and **4** is based on the value of *J*(7,8) (9.0 and 3.7, respectively).

We evaluated the inhibitor **4** against both human *O*-GlcNAcase and *Bt*GH84 (Table 1), and found in both cases a clear pattern of competitive inhibition (Fig. 2 and supporting material). Somewhat surprisingly, despite its obvious structural relationship to PUGNAc **1**, the inhibitor is not as potent as PUGNAc with either enzyme. In light of these results we considered that the

**Table 1** Inhibition constants for inhibitors and enzymes studied

| Inhibitor | *O*-GlcNAcase $K_I$ (μM) | *Bt*GH84 $K_I$ (μM) | β-Hexosaminidase $K_I$ (μM) |
|---|---|---|---|
| PUGNAc | 0.05[5,8] | 0.01[6] | 0.05[8] |
| LOGNAc | 1.7[5] | ND[a] | ND[a] |
| *gluco*-nagstatin | 0.42[b] | 0.50[b] | 0.01[10] |
| PUGNAc–imidazole hybrid | 3.8 | 3.9 | ND[a] |

[a] ND: Not determined. [b] Determined by Dixon analysis.

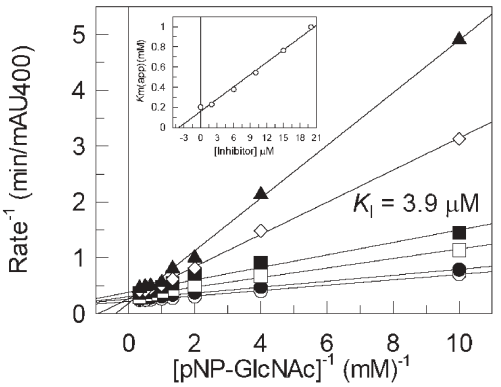


**Fig. 2** Inhibition of *Bt*GH84-catalyzed hydrolysis of MU-GlcNAc by PUGNAc–imidazole hybrid inhibitor (**4**) shows a pattern of competitive inhibition. The concentrations of the inhibitor used (μM) were 20.0 (▲), 15.0 (◇), 10.0 (■), 6.00 (□), 2.00 (●), and 0.00 (○). Inset, analysis of $K_I$ from plotting $K_M$ apparent against the inhibitor concentration.

*N*-phenylcarbamoyl substituent may not be as favourable a substituent in pyridoimidazole-type inhibitors of family 84 *O*-GlcNAcases as suggested by the formal analogy of **4** to PUGNAc. Alternatively, the conformational rigidity imposed by the ring system may not allow this type of inhibitor to adopt a conformation that is either sufficiently close to that of the transition state or one which maximises adventitious interactions with the enzyme. The *gluco*-configured analogue of nagstatin (**3**), previously prepared by us,[10] was also assayed against both human *O*-GlcNAcase and *Bt*GH84 (Table 1). *gluco*-Nagstatin **3**, indeed, shows potency similar to our PUGNAc–imidazole hybrid **4** as well as to LOGNAc **2**, suggesting that the enforced rigidity of the imidazole ring of hybrid **4** mitigates the advantage provided by the phenyl ring substituent.

To gain a more detailed understanding of the molecular basis for these differences, we determined the three-dimensional structure of *Bt*GH84 in complex with the PUGNAc–imidazole analogue **4** (PDB code 2j47, Fig. 3A) at 1.97 Å resolution and compared this structure to that of PUGNAc **1** bound to the *Clostridium perfringens* homologue (*Cp*GH84H) (Fig. 3B).[9] The piperidinose ring adopts an approximate $^4H_3$ conformation similar to that seen for PUGNAc (Fig. 3B) in complex with *Cp*GH84H. An overlay of this model with one determined[9] earlier for PUGNAc in complex with *Cp*GH84H, however, reveals several differences. The most notable stems from the conjugated π-system of the imidazole ring that extends into the pendant amide group. This orbital overlap favours an orientation of the amide group that is in plane with the imidazole and, as a consequence, forces the phenyl group into a position that differs from that observed for PUGNAc (Fig. 3). In this position, the phenyl ring of the PUGNAc–imidazole hybrid is more solvent exposed than the phenyl ring of PUGNAc bound to *Cp*GH84H and makes fewer productive contacts with the enzyme. This positioning of the phenyl group also forces Trp286 out of the position found for the uncomplexed enzyme (Fig. 3A). The amide carbonyl of the PUGNAc–imidazole hybrid is also "flipped" the opposite way compared to the PUGNAc complex of *Cp*GH84H. One consequence of this rotation is that the carbonyl group of the amide does not form any hydrogen bonds with the enzyme, a situation that is not seen for PUGNAc when bound to *Cp*GH84H

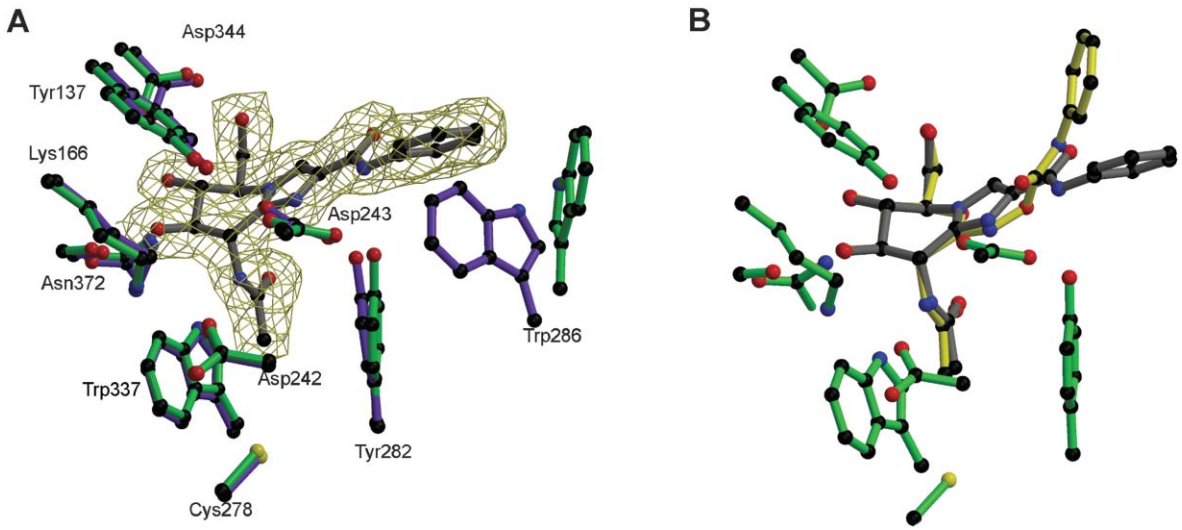


**Fig. 3** **A**. Observed electron density ($2F_{obs} - F_{calc}$ at $1\sigma$) for the PUGNAc–imidazole hybrid (**4**) bound to *Bt*GH84. Residues of the protein are shown in green with the positions of the equivalent side-chains from the native enzyme structure in purple. **B**. An overlay of the *Bt*GH84 PUGNAc–imidazole hybrid complex with the *Cp*GH84H (PUGNAc moiety only shown in yellow) PUGNAc complex. This figure was drawn using BOBSCRIPT.[19]

which instead forms a hydrogen bond with the catalytic acid, Asp398, of that enzyme.[9]

These observations provide insight into the relative $K_I$ values determined for PUGNAc–imidazole and *gluco*-nagstatin with *O*-GlcNAcase. The differences in $K_I$ values between LOGNAc and PUGNAc likely stem from the presence of the *N*-phenyl carbamoyl group. The PUGNAc–imidazole hybrid, which has a similar $K_I$ value to LOGNAc, is bound with the phenyl group oriented differently such that it does not efficiently capture available binding energy. Interestingly, *gluco*-nagstatin is a 40-fold poorer inhibitor toward the family 84 human *O*-GlcNAcase as compared to the family 20 β-hexosaminidase. The structural basis for this difference in affinities is difficult to account for but may arise from differences in the acidity of the enzymic general catalytic acid. *gluco*-Nagstatin binds 3-fold better than LOGNAc itself and so the tetrahydroimidazopyridine scaffold offers an equally potent, yet stable, scaffold on which to graft substituents conferring improved potency when the constraints of decreased flexibility are overcome.

The similarity of the inhibition constants determined for the PUGNAc–imidazole hybrid and *gluco*-nagstatin toward human *O*-GlcNAcase and *Bt*GH84 (Table 1) illustrates the value of this bacterial enzyme as a good model of the human enzyme. Detailed structural analyses of *Bt*GH84 in complex with inhibitors will facilitate the development of still more potent, selective, and stable inhibitors of *O*-GlcNAcase. Collectively, the results obtained here suggest that tetrahydroimidazopyridine-based inhibitors having a more flexible linker region could be more potent than PUGNAc. These inhibitors and further derivatives will be useful molecules, having significantly improved stability, for studying the cellular role of *O*-GlcNAc.

Keith Stubbs and Bruno Bernet are thanked for expert assistance. DJV is a scholar of the MSFHR and a Canada Research Chair in Chemical Glycobiology. We thank the Swiss National Science Foundation, the Natural Sciences and Engineering Research Council of Canada, and the Biotechnology and Biochemical Sciences Research Council for funding.

## Notes and references

‡ For the family classification of glycoside hydrolases see URL: http://afmb.cnrs-mrs.fr/CAZY/.[20]

1 C. R. Torres and G. W. Hart, *J. Biol. Chem.*, 1984, **259**, 3308–3317.
2 L. Wells, K. Vosseller and G. W. Hart, *Science*, 2001, **291**, 2376–2378.
3 J. A. Hanover, *FASEB J.*, 2001, **15**, 1865–1876.
4 K. Vosseller, L. Wells, M. D. Lane and G. W. Hart, *Proc. Natl. Acad. Sci. U. S. A.*, 2002, **99**, 5313–5318.
5 D. L. Y. Dong and G. W. Hart, *J. Biol. Chem.*, 1994, **269**, 19321–19330.
6 R. J. Dennis, E. J. Taylor, M. S. Macauley, K. A. Stubbs, J. P. Turkenburg, S. J. Hart, G. N. Black, D. J. Vocadlo and G. J. Davies, *Nat. Struct. Mol. Biol.*, 2006, **13**, 365–371.
7 D. Beer, J. L. Maloisel, D. M. Rast and A. Vasella, *Helv. Chim. Acta*, 1990, **73**, 1918–1922.
8 M. S. Macauley, G. E. Whitworth, A. W. Debowski, D. Chin and D. J. Vocadlo, *J. Biol. Chem.*, 2005, **280**, 25313–25322.
9 F. V. Rao, H. C. Dorfmueller, F. Villa, M. Allwood, I. M. Eggleston and D. M. van Aalten, *EMBO J.*, 2006, **25**, 1569–1578.
10 M. Terinek and A. Vasella, *Helv. Chim. Acta*, 2005, **88**, 10–22.
11 T. Aoyama, H. Naganawa, H. Suda, K. Uotani, T. Aoyagi and T. Takeuchi, *J. Antibiot.*, 1992, **45**, 1557–1558.
12 P. Ermert and A. Vasella, *Helv. Chim. Acta*, 1991, **74**, 2043–2053.
13 A. Vasella, G. J. Davies and M. Böhm, *Curr. Opin. Chem. Biol.*, 2002, **6**, 619–629.
14 T. D. Heightman and A. T. Vasella, *Angew. Chem., Int. Ed.*, 1999, **38**, 750–770.
15 T. D. Heightman, M. Locatelli and A. Vasella, *Helv. Chim. Acta*, 1996, **79**, 2190–2200.
16 T. D. Heightman, A. Vasella, K. E. Tsitsanou, S. E. Zographos, V. T. Skamnaki and N. G. Oikonomakos, *Helv. Chim. Acta*, 1998, **81**, 853–864.
17 N. Panday, Y. Canac and A. Vasella, *Helv. Chim. Acta*, 2000, **83**, 58–79.
18 A. S. Thompson, G. R. Humphrey, A. M. Demarco, D. J. Mathre and E. J. J. Grabowski, *J. Org. Chem.*, 1993, **58**, 5886–5888.
19 R. M. Esnouf, *J. Mol. Graph. Model.*, 1997, **15**, 132–134.
20 B. Henrissat and A. Bairoch, *Biochem. J.*, 1996, **316**, 695–696.

 